



HAL
open science

Inulin prebiotic reinforces host cancer immunosurveillance via $\gamma\delta$ T cell activation

Emilie Boucher, Caroline Plazy, Mathias L Richard, Antonia Suau, Irène Mangin,
Muriel Cornet, Delphine Aldebert, Bertrand Toussaint, Dalil Hannani

► To cite this version:

Emilie Boucher, Caroline Plazy, Mathias L Richard, Antonia Suau, Irène Mangin, et al.. Inulin prebiotic reinforces host cancer immunosurveillance via $\gamma\delta$ T cell activation. *Frontiers in Immunology*, 2023, 14, pp 1104224. <10.3389/fimmu.2023.1104224>. <hal-04075792>

HAL Id: hal-04075792

<https://cnam.hal.science/hal-04075792v1>

Submitted on 20 Apr 2023

HAL is a multi-disciplinary open access archive for the deposit and dissemination of scientific research documents, whether they are published or not. The documents may come from teaching and research institutions in France or abroad, or from public or private research centers.

L'archive ouverte pluridisciplinaire **HAL**, est destinée au dépôt et à la diffusion de documents scientifiques de niveau recherche, publiés ou non, émanant des établissements d'enseignement et de recherche français ou étrangers, des laboratoires publics ou privés.



Distributed under a Creative Commons CC BY 4.0 - Attribution - International License



OPEN ACCESS

EDITED BY

Fabiana Ourique,
Universidade Federal de Juiz de Fora, Brazil

REVIEWED BY

Shubhada Vivek Chiplunkar,
Research and Education in Cancer, India
Dieter Kabelitz,
University of Kiel, Germany

*CORRESPONDENCE

Dalil Hannani

✉ Dalil.Hannani@univ-grenoble-alpes.fr

SPECIALTY SECTION

This article was submitted to
Cancer Immunity
and Immunotherapy,
a section of the journal
Frontiers in Immunology

RECEIVED 21 November 2022

ACCEPTED 06 February 2023

PUBLISHED 17 February 2023

CITATION

Boucher E, Plazy C, Richard ML, Suau A,
Mangin I, Cornet M, Aldebert D,
Toussaint B and Hannani D (2023) Inulin
prebiotic reinforces host cancer
immunosurveillance via $\gamma\delta$ T cell activation.
Front. Immunol. 14:1104224.
doi: 10.3389/fimmu.2023.1104224

COPYRIGHT

© 2023 Boucher, Plazy, Richard, Suau,
Mangin, Cornet, Aldebert, Toussaint and
Hannani. This is an open-access article
distributed under the terms of the [Creative
Commons Attribution License \(CC BY\)](#). The
use, distribution or reproduction in other
forums is permitted, provided the original
author(s) and the copyright owner(s) are
credited and that the original publication in
this journal is cited, in accordance with
accepted academic practice. No use,
distribution or reproduction is permitted
which does not comply with these terms.

Inulin prebiotic reinforces host cancer immunosurveillance via $\gamma\delta$ T cell activation

Emilie Boucher¹, Caroline Plazy², Mathias L. Richard^{3,4},
Antonia Suau^{1,5}, Irène Mangin⁵, Muriel Cornet²,
Delphine Aldebert¹, Bertrand Toussaint² and Dalil Hannani^{1*}

¹Univ. Grenoble Alpes, CNRS, UMR 5525, VetAgro Sup, Grenoble INP, TIMC, Grenoble, France, ²Univ. Grenoble Alpes, CNRS, UMR 5525, VetAgro Sup, Grenoble INP, CHU Grenoble Alpes, TIMC, Grenoble, France, ³Université Paris-Saclay, INRAE, AgroParisTech, Micalis Institute, Jouy-en-Josas, France, ⁴Paris Center for Microbiome Medicine, Fédération Hospitalo-Universitaire, Paris, France, ⁵USC Cnam-ANSES Metabiot, Conservatoire National des Arts et Métiers, Paris, France

The gut microbiota is now recognized as a key parameter affecting the host's anti-cancer immunosurveillance and ability to respond to immunotherapy. Therefore, optimal modulation for preventive and therapeutic purposes is very appealing. Diet is one of the most potent modulators of microbiota, and thus nutritional intervention could be exploited to improve host anti-cancer immunity. Here, we show that an inulin-enriched diet, a prebiotic known to promote immunostimulatory bacteria, triggers an enhanced Th1-polarized CD4⁺ and CD8⁺ $\alpha\beta$ T cell-mediated anti-tumor response and attenuates tumor growth in three preclinical tumor-bearing mouse models. We highlighted that the inulin-mediated anti-tumor effect relies on the activation of both intestinal and tumor-infiltrating $\gamma\delta$ T cells that are indispensable for $\alpha\beta$ T cell activation and subsequent tumor growth control, in a microbiota-dependent manner. Overall, our data identified these cells as a critical immune subset, mandatory for inulin-mediated anti-tumor immunity *in vivo*, further supporting and rationalizing the use of such prebiotic approaches, as well as the development of immunotherapies targeting $\gamma\delta$ T cells in cancer prevention and immunotherapy.

KEYWORDS

$\gamma\delta$ T cells, immunosurveillance, microbiota, prebiotic, inulin

1 Introduction

According to the World Health Organization (WHO), cancer is the second leading cause of death globally, and the increasing cancer incidence is a major public health issue worldwide (1). Despite the development of innovative treatments, such as immunotherapy, including immune checkpoint blockers (ICB), which have recently revolutionized patient care, quality of life, and survival, huge efforts are still needed to prevent and treat cancers. It is worth noting that between 30% and 50% of cancer deaths can be prevented by modifying or avoiding major risk factors and implementing existing evidence-based prevention strategies, including eating a healthy diet, primarily fruits and vegetables (2). A healthy

diet helps prevent the development of cancer in several ways that may be synergistic. It limits host cell oxidation and metabolism as well as genetic instability and chronic inflammation. It also affects gut microbiota composition and functions, and subsequently, host immune functions (3).

Indeed, the host immune tonus is a key parameter in cancer prevention through immunosurveillance, which relies on the ability of different immune cell subsets to patrol, recognize, and eliminate transformed cells (4). Both innate and adaptive immunity participate in this process and prevent cancer development by recognizing stress-induced ligands, dysregulation of tumor cell metabolism, or peptides derived from tumor antigens. Effector CD8⁺ T cells are among the most important subsets involved in cancer surveillance and are key targets in immunotherapy. Furthermore, $\gamma\delta$ T cells are unconventional T cells representing a unique population displaying multiple functions, including potent anti-tumor activity (5, 6). Indeed, $\gamma\delta$ T cells are key players in cancer immunosurveillance, as they can recognize transformed cells expressing stress-ligands *via* innate receptors (e.g. NKG2D) or metabolic products derived from dysregulated tumors (e.g. mevalonate pathway). When activated, $\gamma\delta$ T cells produce pro-inflammatory cytokines, such as interferon γ (IFN γ), which in turn promote anti-cancer CD8⁺ T cell immunity. They can also directly kill cancer cells *via* perforin/granzyme mediated cytotoxicity. Therefore, $\gamma\delta$ T cell infiltration within the tumor bed is a favorable prognostic marker in several human cancers (7, 8) and represents a promising target in cancer immunotherapy (9, 10).

A growing body of evidence has also highlighted that the gut microbiota may have a positive impact on cancer prevention or treatment, especially *via* improved host immunosurveillance of cancer (11, 12) as well as patients' ability to respond to chemotherapy (13) or immunotherapy (11, 14–16). These seminal studies have identified certain families, genera, or species of bacteria associated with the gut microbiota that appear to correlate with a strong host immune status and a subsequent favorable response to cancer therapy. For instance, *Bifidobacterium*, *Ruminococcaceae*, *Akkermansia muciniphila*, *Enterococcus irae*, and *Allistipes* have all been positively associated with ICB responses. As preclinical proof of concept, it has been shown that either Fecal Microbiota Transplantation (FMT) from responding patients or direct supplementation with immunostimulatory bacteria can restore the ability to respond to ICB in mice (14, 15). Taken together, these studies strongly suggest that modulation of the gut microbiota may represent a major strategy to prevent and/or treat cancers by optimizing host immunity and subsequent anti-tumor responses.

It is noteworthy, 70% of host immune cells are located within the gut, close to microbiota-derived signals (17). Among the Intra Epithelial Lymphocytes (IELs) in the gut, the $\gamma\delta$ T cells represent the largest immune subset. Interestingly, their early development is largely dependent on gut microbiota after birth (18). Unlike conventional $\alpha\beta$ TCR⁺ CD4⁺ or CD8⁺ T cells, which recognize antigen-derived peptides, these cells recognize metabolic products derived from bacteria or tumor cells (19, 20).

Diet is probably the most powerful microbiota modulator, in terms of both its composition and metabolic functions (21). Thus, modulation of the gut microbiota by nutritional intervention,

particularly *via* prebiotics, could be of great interest in optimizing host immune responses, including cancer immunosurveillance. Prebiotics are defined as non-digestible food ingredients that benefit the host by selectively stimulating the growth and activity of one species or a limited number of bacterial species in the colon (22). Among the prebiotics, inulin, a Fructo-Oligo Saccharide derived from chicory roots, is well known to promote some colonic bacteria, including *Bifidobacterium*, which has been associated with optimal host immunity in the context of cancer immunosurveillance and immunotherapy (11, 23). Recently, the use of inulin to stimulate immunosurveillance was confirmed by Li et al., who showed that an inulin diet attenuated tumor growth in a CD8⁺ T cell-dependent manner in mice (24). To date, the effect of nutritional intervention on systemic immunity, including the anti-tumor CD8⁺ T cell response, remains largely unknown.

Since an inulin-enriched diet is known to alter the metabolic activity of the gut microbiota (25), we hypothesized that intestinal and systemic $\gamma\delta$ T cells might subsequently be altered. In the present study, we examined the role of $\gamma\delta$ T cells in inulin-mediated anti-tumor effects and highlighted their pivotal role in CD8⁺ T cell-mediated immunosurveillance in several transplantable mouse tumor models.

2 Results

2.1 Inulin-enriched diet leads to potent tumor growth control and enhanced $\gamma\delta$ Tumor Infiltrated Lymphocytes activity

Inulin has been described as a promoter of immunostimulatory bacteria associated with strong anti-tumor immunity (11, 26). Therefore, we evaluated whether 15 days of preconditioning in WT mice by adding inulin to drinking water could promote host anti-tumor immunity after subcutaneous injection of a syngeneic B16-OVA melanoma tumor (Figure 1A). Consistent with a previous study in another tumor model (24), inulin strongly attenuated aggressive B16-OVA melanoma tumor growth (Figure 1B left panel). Notably, the inulin-mediated anti-tumor effect was also confirmed in other tumor models (i.e., MCA205 fibrosarcoma and MC38 colorectal cancer cell lines, Figure 1B middle and right panel). To better understand the mechanisms behind these observations, we analyzed the Tumor Infiltrating Lymphocytes (TILs) when the control diet group reached maximum ethical tumor size (day 13 post B16-OVA tumor inoculation, Figure 1A). Flow cytometry analyses revealed that inulin triggered greater infiltration of immune cells (CD45⁺ cells) within the tumor bed (Figure 1C) as well as greater tumor infiltration of dendritic cells (Figure S1). Consistent with the anti-tumor activity observed (Figure 1B), we found that the inulin-enriched diet triggered a potent Th1 anti-tumor response, as illustrated by the greater amount of IFN γ -producing CD4⁺ and CD8⁺ TILs (Figures 1D, E). In agreement with this, immunization with OVA protein adjuvanted with PolyI:C (a Th1 polarizing adjuvant) led to a higher frequency of OVA-specific CD8⁺ T cells in the lymph nodes of inulin-supplemented mice (Figure S2). This suggests that inulin potentiated the Th1 polarizing activity of PolyI:C.

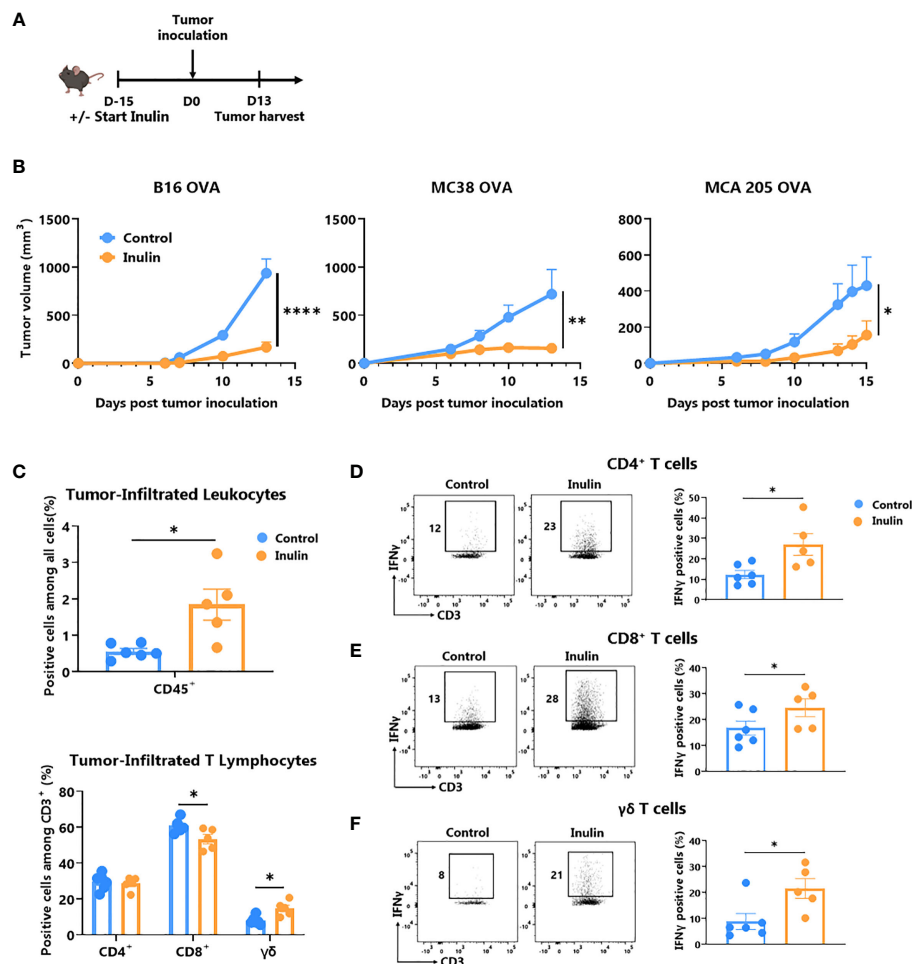


FIGURE 1

Inulin-enriched diet inhibits tumor growth and reinforces tumor-infiltrated immunity. (A) Experimental schedule. C57BL/6 mice were fed with a control or an inulin-enriched diet (7.2% in drinking water) ($n=6$ mice per group) starting 15 days before subcutaneous (s.c.) inoculation of 2×10^5 B16 OVA melanoma cells, or 5×10^5 MC38 OVA colorectal cancer cells, or 2×10^5 MCA 205 OVA fibrosarcoma cells ($n=6$ mice per group). (B) Tumor growth curves of mice treated as described in (A) and implanted with indicated tumors. (C) Frequency of B16 OVA tumor-infiltrated total CD45⁺ and effector CD4⁺, CD8⁺ or $\gamma\delta$ TcR⁺ T Lymphocytes from mice treated as described in (A) when control tumors reached the maximal ethic size. (D–F) Frequency of B16 OVA tumor-infiltrated IFN γ -producing cells gated on CD45⁺ CD3⁺ $\gamma\delta$ TcR⁻ CD4⁺, defined as CD4⁺ T cells (D), CD45⁺ CD3⁺ $\gamma\delta$ TcR⁻ CD4⁻, defined as CD8⁺ T cells (E) or CD45⁺ CD3⁺ $\gamma\delta$ TcR⁺, defined as $\gamma\delta$ T cells (F) from mice treated as in (A). Graphs show the mean \pm SEM. Statistically significant results are indicated by: * $p < 0.05$, ** $p < 0.005$, **** $p < 0.0001$ by two-way ANOVA with Geisser Greenhouse's correction (B) or by Mann-Whitney tests (C–F).

In addition, we assessed the frequency and activity of $\gamma\delta$ TILs, and found that inulin-enriched diet also promoted $\gamma\delta$ TIL infiltration (Figure 1C) and IFN γ -production in residual tumors (Figure 1F). Notably, among both MCA205 and MC38 TILs, only $\gamma\delta$ T cells infiltration was significantly increased under the inulin diet (Figure S3). Taken together, these data indicate that inulin triggered greater tumor infiltration by immune cells, potent Th1-polarized anti-tumor immunity, and in particular, high IFN γ production by conventional T cells as well as $\gamma\delta$ TILs, which may ultimately lead to tumor growth control.

2.2 Inulin-mediated anti-tumor immunity relies on $\gamma\delta$ T cell

$\gamma\delta$ T cells are unconventional T cells recognizing metabolic-related molecules such as phosphoantigens, and represent an

interesting target/tool in cancer immunotherapy because they exhibit potent anti-tumor activity (6). As tumor infiltration and IFN γ production are enhanced by an inulin-enriched diet, we evaluated whether these cells could play a central role in inulin-mediated anti-tumor immunity. To assess their contribution, we used repeated injections of $\gamma\delta$ TcR-blocking antibody starting the day before the tumor implantation (Figure 2A). Of note, while inulin-treated mice well-controlled tumor growth at day 13, after implantation, administration of $\gamma\delta$ TcR-blocking antibody completely abrogated the inulin-mediated anti-tumor effect (Figure 2B). Interestingly, analysis of TILs revealed that under systemic $\gamma\delta$ T cell blockade, the inulin-enriched diet failed to trigger greater IFN γ -production by CD4⁺ and CD8⁺ TILs (Figures 2C, D). Furthermore, under $\gamma\delta$ TcR blockade and despite the inulin diet, the frequency of IFN γ -producing $\gamma\delta$ TILs was similar to that of the control group, suggesting that $\gamma\delta$ TcR

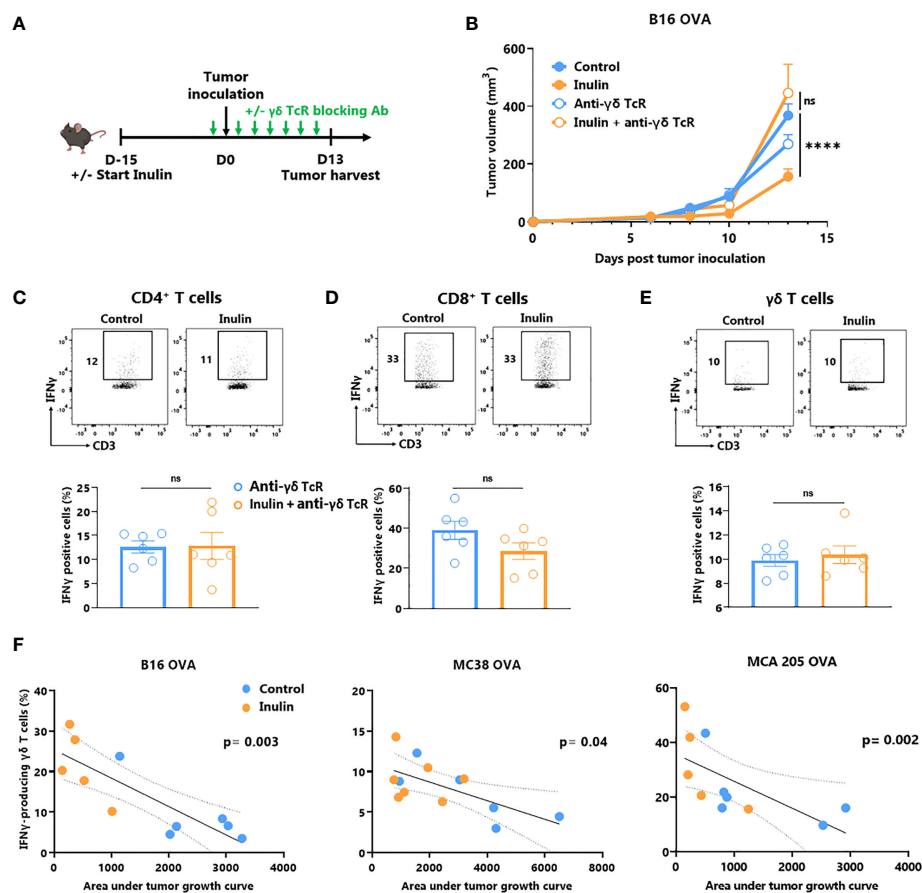


FIGURE 2

Inulin-triggered anti-tumor effect depends on $\gamma\delta$ T lymphocytes. (A) Experimental schedule. C57BL/6 mice were fed with a control diet or inulin-enriched diet (7.2% in drinking water) ($n=12$ mice per group) starting 15 days before s.c. inoculation of 2×10^5 B16 OVA melanoma cells. Anti- $\gamma\delta$ TcR antibodies were injected intraperitoneally (i.p.) to 6 mice per group every two days starting the day before tumor inoculation. (B) Tumor growth curves of mice treated as described in (A). (C–E) Frequency of B16 OVA tumor-infiltrated IFN γ -producing cells gated on CD45+ CD3+ $\gamma\delta$ TcR- CD4+, defined as CD4 $^+$ T cells (C), CD45+ CD3+ $\gamma\delta$ TcR- CD4-, defined as CD8 $^+$ T cells (D) or CD45+ CD3+ $\gamma\delta$ TcR+, defined as $\gamma\delta$ T cells (E) from mice treated as described in (A) when control tumors reached the maximal ethic size. (F) Correlation between IFN γ -producing $\gamma\delta$ T cell infiltration in tumors and the tumor growth in mice fed on a control or inulin-enriched diet ($n=6$ mice per group), bearing the indicated tumor. (A–E) Graphs show the mean \pm SEM, and (F) IFN γ -producing $\gamma\delta$ T cell infiltration in the tumor depending to the tumor growth. ns = not-significant, **** $p < 0.0001$ by two-way ANOVA with Geisser greenhouse's correction (B), by Mann-Whitney tests (C–E), or Spearman test (F).

signaling is required in inulin-mediated immunoactivation (Figure 2E). Taken together, these data indicate that $\gamma\delta$ T cells, and most likely their TcR engagement, are mandatory for inulin-mediated anti-tumor effects. In addition, we observed a significant correlation between the level of tumor infiltration of IFN γ -producing $\gamma\delta$ T cells and tumor growth in all three tumor models (Figure 2F), confirming their pivotal role in inulin-mediated anti-tumor effects.

2.3 Inulin-enriched diet leads to gut-associated $\gamma\delta$ T cell activation and gut inflammation

It is well known that the gut microbiota affects local (gut) and systemic immune tone (27). Since $\gamma\delta$ T cells represent the most abundant immune cell population within the gut epithelium (28), we evaluated the impact of the inulin diet on IFN γ -production by

gut-associated immune cells as well as on the level of gut epithelium inflammation. For this purpose, we collected intestines from mice following a 15-day inulin diet (Figure 3A). The fractions of Intra Epithelial Lymphocytes (IELs) and Lamina Propria Cells (LPCs) were analyzed using flow cytometry. Under inulin, while the frequency of IFN γ -producing CD4 $^+$ and CD8 $^+$ T cells was comparable to that of the control group in IELs and LPCs (Figures 3B, C; Figure S4A, respectively), $\gamma\delta$ T cell IELs showed a higher proportion of IFN γ -producing cells (Figure 3D).

To further characterize inulin-mediated intestinal inflammation, we sorted the epithelial (CD45-) fraction from LPCs (CD45 $^+$) to perform RT-qPCR on genes involved in inflammation, tissue repair, and tight junctions (Figures 3E–G; Figure S5; Table S2). Of the 19 analyzed genes, three inflammation-related genes were significantly upregulated under the inulin regime in epithelial cells, namely Tumor Necrosis Factor (TNF)- α , Cyclo-Oxygenase (Cox)-2 and Matrix Metalloprotease (MMP)-9 (Figure 3F). In the CD45 $^+$ compartment (LPCs), inulin

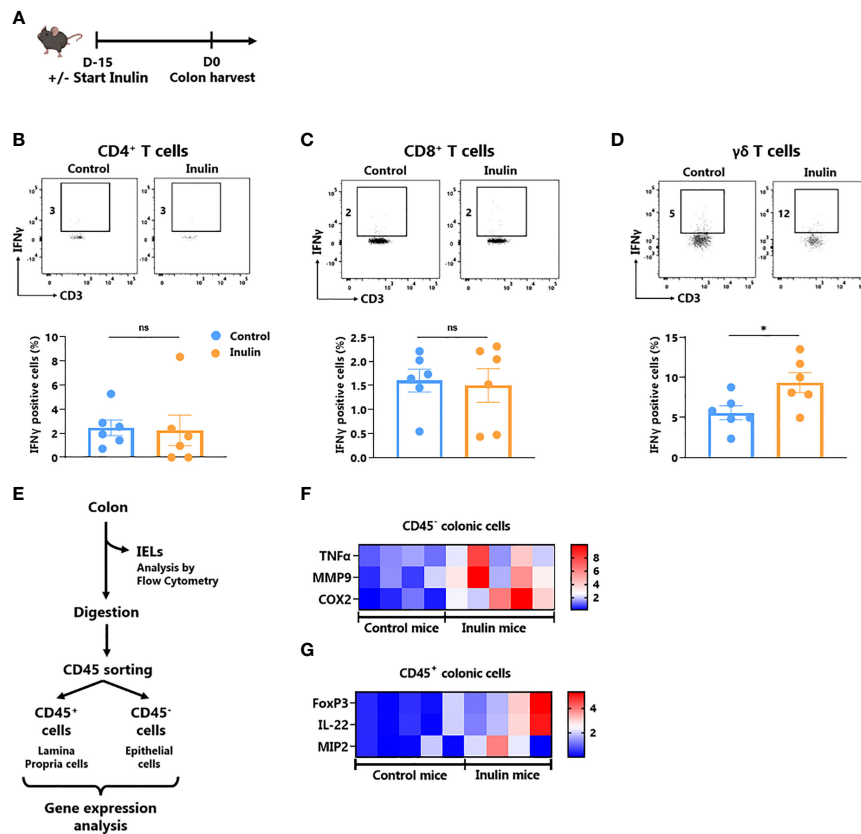


FIGURE 3

Inulin consumption promotes $\gamma\delta$ T IELs and mucosa cell activation in the colon (A) Experimental schedule. C57BL/6 mice were fed with a control diet or inulin-enriched diet (7.2% in drinking water) ($n=12$ mice per group) for 15 days before the analysis of their gut immunity. (B–D) Frequency of IFN γ -producing IntraEpithelial Lymphocytes (IELs) gated on CD45⁺ CD3⁺ $\gamma\delta$ TcR⁻ CD4⁺, defined as CD4⁺ T cells (B), CD45⁺ CD3⁺ $\gamma\delta$ TcR⁻ CD4⁻, defined as CD8⁺ T cells (C) or CD45⁺ CD3⁺ $\gamma\delta$ TcR⁺, defined as $\gamma\delta$ T cells (D) from mice treated as described in (A). (E) Experimental plan of colon treatment after harvest. After isolation of IELs, remaining colon pieces were digested before sorting of CD45⁻ and CD45⁺ cells for further analysis. (F, G) qRT-PCR analysis of inflammation, tissue repair and tight junction -related genes in (F) CD45⁻ and (G) CD45⁺ colon cells sorted as described in (E). (B–D) Graphs show the mean \pm SEM. ns = not-significant, * $p < 0.05$ by Mann-Whitney tests (B–D). (F, G) Graphs show the expression levels of significantly increased genes ($p < 0.05$ by Mann-Whitney test).

triggered significant overexpression of Macrophage Inflammatory Protein (MIP)-2, Interleukin (IL)-22 and the transcriptional factor Forkhead Box P (FoxP)-3 (Figure 3G). Similarly, we observed a trend toward higher IL-10 production, although not significant, by LPC-associated T cells (Figure S4B). Altogether, these results indicate that inulin diet triggered both targeted $\gamma\delta$ T cell activation in IELs and inflammation in gut epithelial cells, in parallel with tissue repair signaling and tolerance induction in the lamina propria.

2.4 Inulin-enriched diet alters the gut microbiota and promotes *Bifidobacterium* growth

To establish a link between the observed intestinal immune activation (Figure 3) and the inulin-enriched diet, we characterized the composition of fecal bacterial microbiota after inulin administration using 16S rDNA sequencing. Metagenomic analysis indicated that five phyla composed the microbiota of these mice: *Firmicutes* (58% of the sequences), *Bacteroidota* (37%

of the sequences), *Desulfobacterota* (1.3% of the sequences), *Proteobacteria* (1.2% of the sequences), and *Actinobacteriota* (2.4% of the sequences). A 15-day inulin diet profoundly altered the gut microbiota composition, as revealed by the relative abundance of these bacterial phyla observed in inulin-treated mice compared to control mice (Figure 4A), with a visible increase in bacteria of the *Actinobacteriota* phylum, and more precisely to the genus *Bifidobacterium*. This diet altered the alpha diversity; the total number of species was not significantly different (387 ± 53 Operational Taxonomic Units (OTUs) for the control group and 378 ± 43 for the inulin group), but the distribution of sequences within the OTUs was significantly different (Shannon index, $p = 0.00582$). A Bray-Curtis β -diversity analysis illustrated by Principal Component Analysis (PCoA) representation confirmed a significant clustering of the overall bacterial microbiota with a p -value < 0.001 (Figure 4B). To identify whether particular bacteria were potentially involved in anti-tumor immunity, we performed differential abundance correlation using a linear discriminant analysis (LDA) effect size algorithm (LefSe; see Material and Methods). The LDA scores plotted in a phylogenetic cladogram showed significant differences across several taxonomic ranks

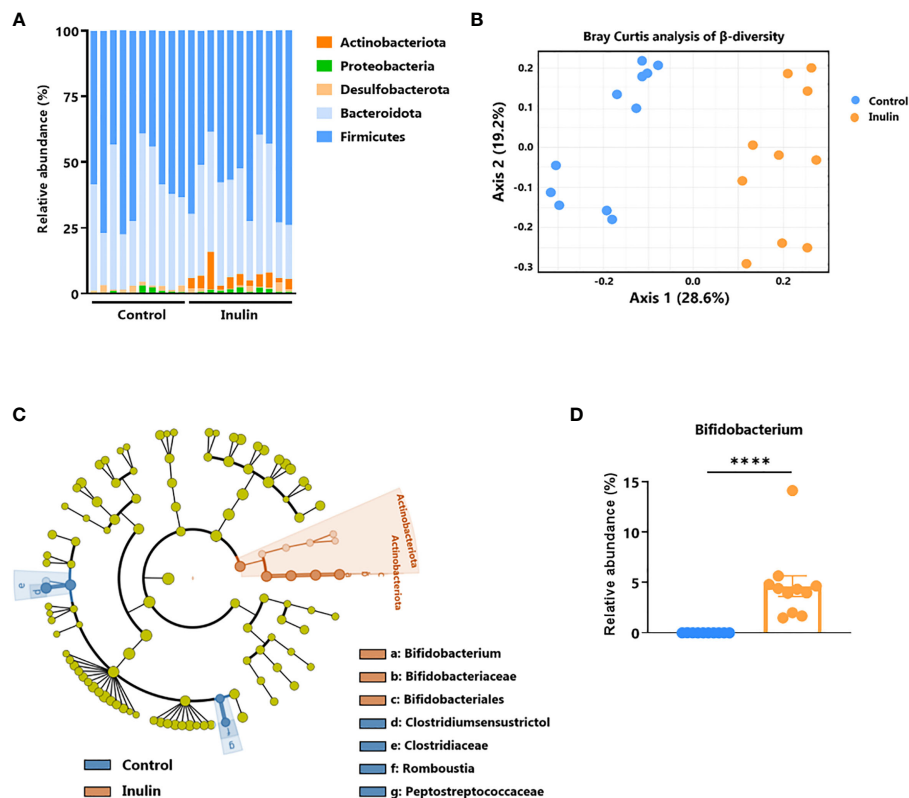


FIGURE 4

Inulin modulates gut microbiota and promotes *Bifidobacterium* growth. Feces from C57BL/6 mice fed with a control (n=10 mice) or an inulin-enriched diet (7.2% in drinking water) (n=11 mice) for 15 days were collected and analysed by 16S rDNA sequencing. (A) Relative abundance of bacterial phyla (B) Bray-Curtis analysis of β -diversity, (C) cladogram representation of Linear discriminant analysis Effect Size (LEfSe) analysis, and (D) relative abundance of *Bifidobacterium* genus. The graph shows the mean \pm SEM. ****p < 0.00001 by Mann-Whitney test.

(Figure 4C). One of the strongest signals, LDA score >4, was the increase in *Bifidobacterium animalis* subsp. *animalis*, a member of the *Actinobacteriota* phylum, in inulin treated mice (4.67%), compared with control mice (0.03%) (Figure 4D; Table S1). Importantly, consistent with our results, *Bifidobacterium* has been shown to exhibit immunostimulatory properties in the context of cancer immunosurveillance and immunotherapy (11, 23). Therefore, *Bifidobacterium* may be involved in the stimulation of inulin-mediated anti-tumor immunity. The second most significant signal concerned the family Clostridiaceae, and in particular, the genus *Clostridium sensu stricto 1*. Our sequences were close to those of *Clostridium saudiense*, *Clostridium disporicum*, and *Clostridium celatum* (these species have nearly identical 16S rDNA sequences). This OTU statistically decreased in the mice microbiota due to treatment, from 6% in the control group to 0,09% in the inulin group (data not shown).

2.5 Inulin-mediated increased anti-tumor immunity relies on gut microbiota

Inulin, a polysaccharide molecule, has been shown to possess adjuvant properties *in vivo* (29, 30). Such direct immune activation may be responsible for the anti-tumor immunity observed under

the inulin regime. To address this issue, we administered a broad-spectrum antibiotic cocktail to the mice 2 days before the inulin diet to significantly reduce the number of bacteria in their gut, as previously described (13) (Figure 5A). After tumor implantation, we observed that concomitant antibiotic treatment completely abolished the ability of inulin to attenuate tumor growth (Figure 5B). Furthermore, inulin failed to trigger a higher frequency of IFN γ -producing $\gamma\delta$ TILs and subsequent CD4 $^+$ and CD8 $^+$ TILs (Figures 5C–E). Altogether, these findings indicate that inulin-mediated anti-tumor activity cannot be attributed to a direct adjuvant effect; rather, it relies on host immune activation mediated by the gut microbiota.

Because $\gamma\delta$ T cells are obligatory for inulin-mediated anti-tumor immunity (Figure 2), and that $\gamma\delta$ T IELs are the only T cell subset activated by inulin diet in the gut (Figure 3), we hypothesized that $\gamma\delta$ TILs could have an intestinal origin. To address this question, we analyzed the expression of the gut-homing chemokine receptor CCR9 in circulating δ T and $\gamma\delta$ TILs. Whereas the number of CCR9-expressing $\gamma\delta$ T decreased in the blood (Figure 5F), their frequency tended to increase in the tumor bed, despite a possible loss of expression in this environment (Figure 5G). Notably, under a concomitant inulin diet and antibiotic treatment, $\gamma\delta$ TILs expressed similar levels of CCR9 compared with the control group (Figure 5H). Taken together,

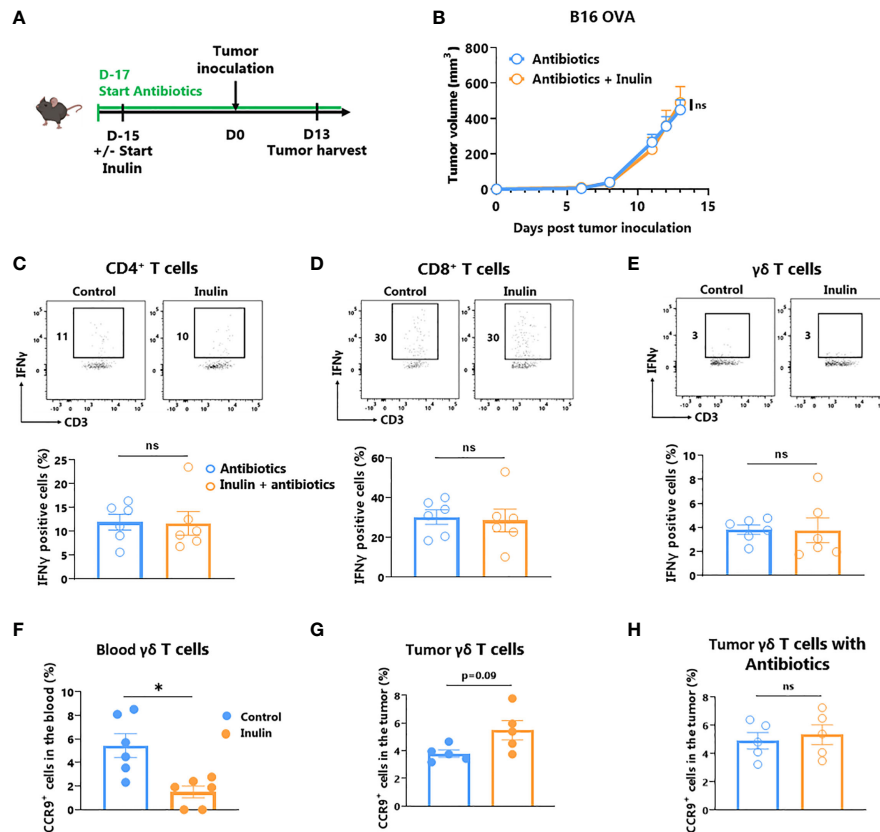


FIGURE 5

Inulin-triggered anti-tumor effect relies on intact bacterial gut microbiota. (A) Experimental schedule. C57BL/6 mice were fed with a control diet or inulin-enriched diet (7.2% in drinking water) ($n=6$ mice per group) starting 15 days before s.c. inoculation of 2×10^5 B16 OVA melanoma cells. Microbial gut microbiota was depleted from 2 days before the beginning of the diet by adding vancomycin (0.25 g/L), colimycin (12×10^6 U/L), ampicillin (1 g/L) and streptomycin (5 g/L) to drinking water. (B) Tumor growth curves of mice treated as described in (A). (C–E) Frequency of B16 OVA tumor-infiltrated IFN γ -producing cells gated on CD45 $^+$ CD3 $^+$ $\gamma\delta$ TCR $^-$ CD4 $^+$, defined as CD4 $^+$ T cells (C), CD45 $^+$ CD3 $^+$ $\gamma\delta$ TCR $^-$ CD4 $^-$, defined as CD8 $^+$ T cells (D) or CD45 $^+$ CD3 $^+$ $\gamma\delta$ TCR $^+$, defined as $\gamma\delta$ T cells (E) from mice treated as described in (A). (F, G) Frequency of CCR9 $^+$ cells among CD45 $^+$ CD3 $^+$ $\gamma\delta$ TCR $^+$ in (F) the blood and in (G) the tumor of mice fed with a control diet or inulin-enriched diet (7.2% in drinking water) ($n=6$ mice per group) starting 15 days before s.c. inoculation of B16 OVA melanoma cells. (H) Frequency of CCR9 $^+$ cells among CD45 $^+$ CD3 $^+$ $\gamma\delta$ TCR $^+$ in tumor of mice treated as described in (A). Graphs show the mean \pm SEM. ns = not-significant, * $p < 0.05$ by two-way ANOVA with Geisser greenhouse's correction (B) or by Mann-Whitney tests (C–H).

these data suggest that inulin-induced activated $5\gamma\delta$ TILs may be of intestinal origin.

2.6 Inulin-enriched regimen is as efficient as α PD-1 Immunotherapy

A large body of evidence suggests that certain immunostimulatory bacteria, including *Bifidobacterium*, may facilitate the efficacy of immune checkpoint inhibitors, including those targeting the anti-PD1/PD-L1 axis (11, 14–16). Because the inulin diet altered the gut microbiota (Figure 5) and favored *Bifidobacterium* (Figure 4), we evaluated whether this diet could be synergistic with anti-PD1 treatment (Figure 6A). Tumor growth monitoring indicated that inulin alone allowed tumor growth control to the same extent as anti-PD-1 alone or in combination (Figure 6B). The individual mouse curves clearly showed that inulin alone triggered the strongest anti-tumor effect compared with anti-PD1 alone or in combination (Figure 6C). TILs analysis revealed

that inulin led to a greater IFN γ production by $\gamma\delta$ T cells (Figure 6D) and CD4 $^+$ cells (Figure 6E), compared with anti-PD1 alone. The combination did not potentiate this effect despite similar PD-1 expression among the TILs (Figure S6). Anti-PD1 immunotherapy reinvigorates CD8 $^+$ TILs and increases their ability to produce IFN γ (31). In agreement with this, anti-PD1 treatment led to a higher proportion of IFN γ -producing CD8 $^+$ TILs within the tumor bed (Figure 6F). Interestingly, inulin alone triggered the activation of CD8 $^+$ TILs, at least to a similar extent.

3 Discussion

Gut microbiota is emerging as a powerful host immune modulator that can be exploited for both cancer prevention and treatment. Consequently, there is an urgent need to understand the cellular and molecular mechanisms that govern this modulation to rapidly translate these findings into innovative preventive or therapeutic strategies.

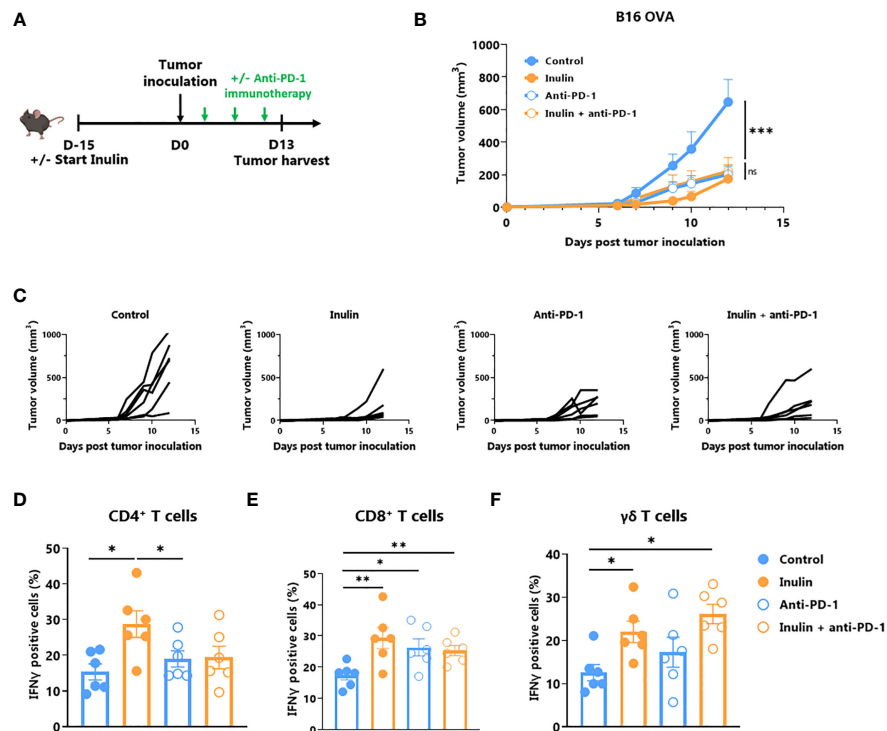


FIGURE 6

Inulin treatment is as efficient as anti-PD-1 immunotherapy. (A) Experimental schedule. C57BL/6 mice were fed with a control diet or inulin-enriched diet (7.2% in drinking water) ($n=12$ mice per group) starting 15 days before s.c. inoculation of 2×10^5 B16 OVA melanoma cells. Anti-PD-1 immunotherapy was injected i.p. to 6 mice per group on days 4, 7 and 10 post-tumor inoculation. (B) Mean and (C) individual tumor growth curves of mice treated as described in (A). (D–F) Frequency of B16 OVA tumor-infiltrated IFN γ -producing cells gated on CD45⁺ CD3⁺ $\gamma\delta$ TcR⁻ CD4⁺, defined as CD4⁺ T cells (D), CD45⁺ CD3⁺ $\gamma\delta$ TcR⁻ CD4⁻, defined as CD8⁺ T cells (E) or CD45⁺ CD3⁺ $\gamma\delta$ TcR⁺, defined as $\gamma\delta$ T cells (F) from mice treated as described in (A). Graphs show the mean \pm SEM. ns = not-significant, * $p < 0.05$, ** $p < 0.005$, *** $p < 0.001$ by two-way ANOVA with Geisser greenhouse's correction (B) or by Mann-Whitney tests (D–F).

Prebiotics contribute to the modification of the composition and functions of the microbiota, and subsequently, to the modification of host immunity. The importance of a prebiotic-enriched diet was recently highlighted in humans by Spencer et al., who reported that a fiber-enriched diet positively influenced the response to immunotherapy in melanoma patients (32).

Inulin is a widely consumed prebiotic, either in the diet or as a supplement. Recently, inulin was reported to attenuate transplantable melanoma tumor growth (24) in a CD8⁺ T cell-dependent manner. In the current study, we reported that inulin-enriched diet triggers not only potent $\alpha\beta$ T cell anti-tumor immunity, but also the accumulation and activation of intratumoral $\gamma\delta$ T cell in a microbiota-dependent manner. We emphasized that these cells are indispensable for the increase of IFN γ -producing CD4⁺ and CD8⁺ TILs and subsequent tumor growth control. We also reported that an inulin-enriched diet remarkably alters the composition of the microbiota and, as expected, significantly promotes the selective growth of *Bifidobacterium* species, which are known to be immunostimulatory. Consistent with this, such a diet promotes the activation of $\gamma\delta$ T IELs in the gut and we found that the frequency of CCR9⁺ tumor-infiltrating cells tends to increase, suggesting a possible intestinal origin of $\gamma\delta$ TILs. Interestingly, CCR9-expressing T cells have been shown to contribute to anti-tumor immunity, and their recruitment into the tumor-bed (by CCL25 intratumoral delivery) (33) improves immunotherapy

efficacy. It is now required to study the $\gamma\delta$ T cell subsets that are recruited within the tumor bed, in order to fully understand their origin.

Regarding a possible synergy with immunotherapy, we found that a prophylactic inulin diet was as effective as anti-PD-1 immunotherapy in our setting and that PD-1 expression was equivalent between groups. Because PD-1 expression identifies exhausted T cells only when combined with other inhibitory receptors such as Tim-3, LAG-3, or TIGIT (34), it is possible that PD-1⁺ TILs under inulin were not in an exhausted state, in contrast to TILs in the control group. Furthermore, in our experiment, we only harvested the tumors 13 days after inoculation to characterize the functionality of the TILs, so it is possible that the combination of inulin and anti-PD-1 treatment would prevent later tumor escape compared to anti-PD-1 alone in the B16 melanoma model. To fully address this question, further phenotyping of TILs and prolonged monitoring of tumor growth are required.

To date, how intestinal and/or systemic $\gamma\delta$ T cells are activated by an inulin-enriched diet remains unclear. Since polysaccharides, as inulin, can activate immune cells in a Toll-like Receptor (TLR)-4-dependent manner (29, 30) we first hypothesized that our observations could rely on such recognition. Indeed, TLR agonists are part of strategies used for harnessing $\gamma\delta$ T cells in cancer immunotherapy (35). Of note, while both human $\gamma\delta$ and CD8⁺ T

cells do express TLR-4 and have been shown to respond to LPS stimulation (36), only $\gamma\delta$ T cells actually express TLR-4 in mice (37), where TLR-4 signaling participates to their development (38). Thus, to evaluate if inulin was able to directly trigger $\gamma\delta$ T cells activation and subsequent tumor growth control, we used a large spectral antibiotics cocktail for altering profoundly the microbiota composition, concomitantly to inulin enrichment. Antibiotics totally abrogated inulin-mediated anti-tumor effect, demonstrating that inulin fails to directly activate $\gamma\delta$ T cells *via* TLR-4, rather, its effect is microbiota-mediated. In addition, in this study, we did not use $\gamma\delta$ TcR deficient mice, rather, we choose to use an antibody-mediated $\gamma\delta$ TcR blockade as first line strategy. This appears more “physiological” than KO mice that can develop some compensatory immune mechanisms. Importantly, we observed that $\gamma\delta$ TcR blockade abrogated inulin-mediated enhanced immunosurveillance. Beyond demonstrating that $\gamma\delta$ T cells are obligate mediators, these data highlighted that their activation was TcR-dependent and thus that microbiota-derived $\gamma\delta$ T cell activation signals could be metabolite-mediated. Altogether, these data allow us to propose a scenario in which intestinal $\gamma\delta$ T cells could be activated in a TcR-dependent manner, most likely by metabolites derived from inulin-mediated remodeling of the microbiota and then recirculated to the tumor to promote CD8⁺ T cell anti-tumor activity. If such scenario is validated in mice, a direct translation to humans could appear difficult due to the differences among mouse and human $\gamma\delta$ T cell subsets. However, in humans, blood-circulating $\gamma\delta$ T cells (V γ 9V δ 2) represent a unique subset able to sense metabolic products. We anticipate that they may represent the human target of inulin-mediated immunomodulation.

In this study, we report three transplantable tumor models in which inulin triggered anti-tumor immune responses. As a result, the growth of melanoma, colorectal and fibrosarcoma tumors were attenuated and accompanied by an increased in $\gamma\delta$ T cell infiltration. To fully investigate the impact of nutritional intervention on cancer immunosurveillance mediated by $\gamma\delta$ T cells, the use of more physiological models, such as genetically engineered mouse models or chemically induced cutaneous tumor models (4), may be useful as they allow for the establishment of proper immunoediting, unlike transplantable tumors. Our study reveals the pivotal role of $\gamma\delta$ T cell in inulin-mediated anti-tumor activity; however, their features could be further investigated. Indeed, it would be of great interest to study their activation phenotype, as well as $\gamma\delta$ T cell subset(s) recruited within the tumor bed under inulin diet. Moreover, to better characterize their anti-tumor activity, one can determine if they directly participate in tumor cell lysis (cytotoxic function) and/or provide a help to effector CD8⁺ T cells either as IFN γ -producing cells and/or as APC-like cells.

Despite these limitations, our data provide a proof of concept that intestinal and systemic $\gamma\delta$ T cell functions can be modulated by nutritional intervention. In particular, we identified these cells as a critical immune subset that is mandatory for inulin-mediated anti-tumor immunity and subsequent control of tumor growth *in vivo*. These results further support and rationalize the use of such prebiotic approaches as well as the development of immunotherapies targeting $\gamma\delta$ T cells in cancer prevention and immunotherapy. Notably, determining which bacteria-derived

metabolite(s) is responsible for this activation would be of great interest in developing future postbiotic immunotherapeutic approaches and rapidly translating these findings for cancer prevention and treatment in humans.

4 Material and methods

4.1 Animals

Female C57Bl/6 mice (5 to 6 weeks aged) were provided by Janvier SA Laboratory (Le Genest-Saint-Isle, France) and housed at “Plateforme de Haute Technologie Animale (PHTA)” UGA core facility (Grenoble, France), EU0197, Agreement C38-51610006, under specific pathogen-free conditions, temperature-controlled environment with a 12-h light/dark cycle and ad libitum access to water and diet. Animal housing and procedures were conducted in accordance with the recommendations from the Direction des Services Vétérinaires, Ministry of Agriculture of France, according to European Communities Council Directive 2010/63/EU and according to recommendations for health monitoring from the Federation of European Laboratory Animal Science Associations. Protocols involving animals were reviewed by the local ethic committee “Comité d’Ethique pour l’Expérimentation Animale no.#12, Cometh-Grenoble” and approved by the Ministry of Research (APAFIS#12905-2018010411002729-v5). Mice were distributed in groups according to their diet. For inulin treatment, mice received standard diet and drinking water supplemented with 7.2% inulin starting 15 days before tumor inoculation. Drinking bottles supplemented with inulin were renewed 3 times a week.

4.2 Cell lines

Ovalbuminexpressing B16 melanoma (B16-OVA), MCA 205 fibrosarcoma cell lines (MCA 205 OVA), and MC38 colorectal cancer cell line (MC38 OVA) were kindly provided by Pr. L. Zitvogel, Gustave Roussy (B16-OVA, MCA205-OVA) and C. Fournier, Inserm U1209 (MC38-OVA). B16-OVA and MC38-OVA cell lines were cultured in 10% Fetal Bovine Serum (FBS) (Gibco) Dulbecco’s modified Eagle’s medium (DMEM) (Gibco) complete medium (supplemented with 1% non-essential amino acids, 1 mM sodium pyruvate, 50 U/mL penicillin, and 50 μ g/mL streptomycin (all from Gibco)). MCA 205 OVA cell line was cultured in 10% FBS Roswell Park Memorial Institute (RPMI) complete medium (Gibco). For plasmid selection, G418 (500 μ g/ml, Sigma) and hygromycin B (50 μ g/ml, Sigma) antibiotics were added to B16-OVA/MC38-OVA and MCA 205-OVA cultures, respectively. All cell lines were tested as mycoplasma-free.

4.3 Tumor implantation

Mice received subcutaneous implantation of either 2×10^5 B16-OVA cells, 2×10^5 MCA 205-OVA cells, or 5×10^5 MC38-OVA cells in 100 μ L PBS in the right flank. Once palpable, tumors were

measured using a caliper, and tumor volume was determined using the following formula: $V_{\text{tumor}} = 0.5 \times (\text{width} \times \text{length}^2)$.

4.4 *In vivo* injection of anti- $\gamma\delta$ TCR and anti-PD-1 antibodies

Mice received 100 μg of the monoclonal antibody anti- $\gamma\delta$ TcR (clone UC7-13D5, Bio X Cell) or anti-PD-1 (clone RMP1-14, Bio X Cell) intraperitoneally, in PBS. Anti- $\gamma\delta$ TcR antibodies were injected the day before tumor implantation and then every 2 days until the end of the experiment. Anti-PD-1 immunotherapy was administered on days 4, 7, and 10 after tumor implantation.

4.5 *In vivo* bacterial microbiota depletion

Mouse gut microbiota was depleted using a cocktail of antibiotics diluted in drinking water: Vancomycin 0.25 g/L (Mylan), Colimycin 12 $\times 10^6$ U/L (Medac), Ampicillin 1 g/L (Sigma) and Streptomycin 5 g/L (Sigma), as previously described (13).

4.6 Tumor digestion

Tumors were collected in complete RPMI medium, lacerated with scalpels, and digested with LiberaseTM 2.5 mg/mL (Roche). Finally, tumors were crushed through a 70 μm cell strainer, washed, and resuspended in 10% FBS complete RPMI.

4.7 Colonic IELs and LPCs isolation and CD45^{+/−} cell sorting

Colons were collected in Hank's Balanced Salt Solution without Ca^{2+} and Mg^{2+} (HBSS) (Gibco), then digested twice with 5 mM HEPES, 5 mM EDTA, 1 mM DTT, and 5% FBS, for IELs isolation. remaining colon pieces were then lacerated with scalpels and digested with collagenase VIII 0.5 mg/mL, DNase I 10 U/mL (Sigma), and 5% FBS in complete RPMI for LPCs isolation. Finally, digested colon pieces were crushed through a 70 μm cell strainer, and cells were resuspended in 10% FBS complete RPMI. CD45⁺ and CD45[−] cells from the LPCs cell fraction were sorted using MACS (Miltenyi Biotec) with CD45 microbeads, according to the manufacturer's protocol.

4.8 Lymph node digestion

Lymph nodes were collected in complete RPMI and then crushed through a 70 μm cell strainer. Cells were later suspended in 10% FBS complete RPMI.

4.9 Blood sample preparation

Blood was collected *via* retro-orbital sampling in K2E tubes (BD Medical). After centrifugation, blood pellets were resuspended in 1

mL Red Blood Cell Lysis buffer 1X (Sigma) and washed with 10% FBS complete RPMI.

4.10 Flow cytometry

To allow intracellular labelling of cytokines, cell suspensions were stimulated 4 h at 37°C with 50 ng/mL phorbol 12-myristate 13-acetate (PMA) (Sigma), 1 $\mu\text{g}/\text{mL}$ ionomycin (Sigma), and Golgi StopTM (BD Biosciences). For extracellular labelling, cells were incubated with 200 ng of each antibody. Antibodies targeting extracellular proteins were CD45 (30-F11), PD-1 (RMP1-30) (BD Biosciences), CD3 (17A2), CD4 (GK1.5), CD44 (IM7), CCR9 (9B1), CD11c (N418), CD8a (53-6.7), PD-L2 (24F.10C12), PD-L1 (10F.9G2), MHC-class II (M5/114.5.2), CD80 (16-10A1), CD40 (3/23) (Biolegend), $\gamma\delta$ -TcR (eBioGL3 (GL-3, GL3), and OVA-dextramer (H-2 Kb) (Immudex) (Table S2).

To allow intracellular labelling, cells were first permeabilized using a FoxP3 staining buffer kit (eBioscience). Antibodies targeting intracellular cytokines were IFN γ (XMG1.2) (Biolegend), IL-10 (JES5-16E3) (Thermo Fisher Scientific), and IL-17A (TC11-18H10) (BD Biosciences) (Table S2). After intracellular labelling, cells were fixed and stored using FACS Lysing Solution 1X (BD Biosciences). All data were collected using a BD Biosciences FACSCanto II or Lyric and analyzed using FlowJo software.

4.11 Bacterial DNA extraction and 16S sequencing from mouse feces

Fecal samples were collected and stored at -80°C. DNA was extracted from feces following optimized JJ Godon protocole (39). After nucleic acid precipitation with isopropanol, DNA suspensions were incubated overnight at 4°C and centrifuged at 20,000 \times g for 30 min. The supernatants were transferred to a new tube containing 2 μL of RNase (RNase A, 10 mg/ml; EN0531; Fermentas, Villebon sur Yvette, France) and incubated at 37°C for 30 min. Nucleic acids were precipitated by the addition of 1 ml of absolute ethanol and 50 μL of 3 M sodium acetate and centrifuged at 20,000 \times g for 10 min. The DNA pellets were washed with 70% ethanol 3 times, dried, and resuspended in 100 μL of Tris-EDTA (TE) buffer (10 mM Tris-HCl, 1 mM EDTA, adjusted pH 8). The DNA suspensions were stored at -20°C for 16S rDNA sequence analysis.

4.12 16S sequencing data processing

Bacterial diversity was determined for each sample by targeting a portion of the ribosomal genes. PCR was performed to prepare amplicons using V3-V4 oligonucleotides (PCR1F_460: 5' CTTT CCCTACACGACGCTCTTCCGATCTACGGGAGGCAGCAG 3', PCR1R_460: 5' GGAGTTCAGACGTGTGCTCTTCCGATCT TACCAGGGTATCTAATCCT 3'), with 30 amplification cycles at an annealing temperature of 65°C. Amplicon quality was verified by gel electrophoresis, and PCR products were sent to the @BRIDGE platform for sequencing on an Illumina MiSeq platform (Illumina, San Diego, CA, USA).

The 16S sequences were demultiplexed and quality-filtered using the QIIME version 2.1.0 software package (40). Sequences were analyzed and normalized using the pipeline FROGS (Find Rapidly OTU with Galaxy Solution) (41, 42). PCR primers were removed and sequences with sequencing errors in the primers were excluded. The reads were clustered into Operational Taxonomic Units (OTUs) using the Swarm clustering method. Chimerae were removed, and 580 OTUs were assigned at different taxonomic levels (from phylum to species) using the RDP classifier and NCBI Blast+ on the Silva_138.1_16S database. When needed, the phylogeny was checked using the Phylogeny browser (<https://www.ncbi.nlm.nih.gov/Taxonomy/Browser/wwwtax.cgi>).

35538 reads were randomly selected from each sample to normalize the data. Raw reads were deposited into the SRA database (ID: PRJNA888063). The R packages “Biom” and “Phyloseq” were used for data analysis and plotting (43). Rarefaction analysis was performed to compare the relative abundance of OTUs across samples. Alpha diversity was measured using Observed, Chao1, Shannon, Simpson, and Inverse Simpson indexes. Beta diversity was measured using the Bray–Curtis distance matrix and used to construct principal coordinate analysis (PCoA) plots. The linear discriminant analysis (LDA) effect size (LEfSe) algorithm was used to identify taxa specific to diet and/or treatment (41, 42).

4.13 Real-time quantitative reverse transcription

Total RNA was extracted from IELs and LPCs using the RNEASY-QIAGEN kit, according to the manufacturer’s protocol. The purity and concentration of the extracted RNA were determined by reading the absorbance at 260 and 280 nm using a NanoDrop spectrophotometer (Thermo Fisher). The extracted RNA was then retrotranscribed using the Superscript II kit (Invitrogen). qRT-PCR analysis was performed using SYBR Green Master Mix (Applied Biosystems) and the StepOne™ RealTime PCR system (Thermo Fischer). PCR conditions were: 2 min at 95°C, then 40 cycles of 15 s at 95°C and 1 min at 60°C. The sequence-specific primers used are shown in Table S3 (GAPDH and β 2M primers were from Eurofins Scientific; other primers were from Merck). The expression levels were normalized to GAPDH and β 2M endogenous gene levels, and each value was then compared to a reference sample named the calibrator. Finally, relative quantification (RQ) values were calculated.

Data availability statement

The data presented in the study are deposited in the SRA repository (<https://www.ncbi.nlm.nih.gov/sra/>), accession number PRJNA888063.

Ethics statement

The animal study was reviewed and approved by “Comité d’Ethique pour l’Expérimentation Animale no.#12, Cometh-

Grenoble” and approved by the Ministry of Research (APAFIS#12905-2018010411002729-v7).

Author contributions

DH contributed to conception and design of the study, acquisition and analysis of the data, and grants acquisition. EB contributed to the design of the study and acquisition and analysis of the data. CP contributed to the acquisition and analysis of the data. MR, IM, AS contributed to the analysis and interpretation of the data. DH wrote the first draft of the manuscript. All authors contributed to the article and approved the submitted version.

Funding

This work (DH) was supported by GEFLUC Dauphiné-Savoie, Ligue contre le Cancer Comité Isère, Ligue contre le Cancer Comité Savoie, Université Grenoble Alpes IDEX Initiatives de Recherche Stratégiques. EB is supported by a grant salary from the French Ministry of Higher Education, Research and Innovation. The funders had no role in study design, data collection or analysis.

Acknowledgments

We would like to thank Sylvie Berthier (Cytometry Platform, CHUGA), Dr. Hervé Lerat, Kevin Escot and Laurie Arnaud (PHTA Animal Facility), Clément Caffaratti and Hélène Coradin (TIMC Lab), and Théo Ziegelmeyer (Inserm U1209) for their technical assistance. This work benefited from the facilities and expertise of @BRIDGE for 16S sequencing (Université Paris-Saclay, INRAE, AgroParisTech, GABI, 78350 Jouy-en-Josas, France).

Conflict of interest

The authors declare that the research was conducted in the absence of any commercial or financial relationships that could be construed as a potential conflict of interest.

Publisher’s note

All claims expressed in this article are solely those of the authors and do not necessarily represent those of their affiliated organizations, or those of the publisher, the editors and the reviewers. Any product that may be evaluated in this article, or claim that may be made by its manufacturer, is not guaranteed or endorsed by the publisher.

Supplementary material

The Supplementary Material for this article can be found online at: <https://www.frontiersin.org/articles/10.3389/fimmu.2023.1104224/full#supplementary-material>

References

- World Health Organization - Cancer. Available at: https://www.who.int/health-topics/cancer#tab=tab_1.
- Fadnes LT, Økland J-M, Haaland ØA, Johansson KA. Estimating impact of food choices on life expectancy: A modeling study. *Fontana L editor PloS Med* (2022) 19(2): e1003889. doi: 10.1371/journal.pmed.1003889
- Kapsetaki SE, Marquez Alcaraz G, Maley CC, Whisner CM, Aktipis A. Diet, microbes, and cancer across the tree of life: a systematic review. *Curr Nutr Rep* (2022) 11(3):508–25. doi: 10.1007/s13668-022-00420-5
- Vesely MD, Kershaw MH, Schreiber RD, Smyth MJ. Natural innate and adaptive immunity to cancer. *Annu Rev Immunol* (2011) 29(1):235–71. doi: 10.1146/annurev-immunol-031210-101324
- Liu Z, Eltoum I-EA, Guo B, Beck BH, Cloud GA, Lopez RD. Protective immunosurveillance and therapeutic antitumor activity of $\gamma\delta$ T cells demonstrated in a mouse model of prostate cancer. *J Immunol* (2008) 180(9):6044–53. doi: 10.4049/jimmunol.180.9.6044
- Hayday AC. $\gamma\delta$ T cell update: Adaptate orchestrators of immune surveillance. *J Immunol* (2019) 203(2):311–20. doi: 10.4049/jimmunol.1800934
- Girard P, Charles J, Cluzel C, Degeorges E, Manches O, Plumaz J, et al. The features of circulating and tumor-infiltrating $\gamma\delta$ T cells in melanoma patients display critical perturbations with prognostic impact on clinical outcome. *Oncoimmunology* (2019) 8(8):e1601483 1–16. doi: 10.1080/2162402X.2019.1601483
- Gentles AJ, Newman AM, Liu CL, Bratman SV, Feng W, Kim D, et al. The prognostic landscape of genes and infiltrating immune cells across human cancers. *Nat Med* (2015) 21(8):938–45. doi: 10.1038/nm.3909
- Saura-Esteller J, de Jong M, King LA, Ensing E, Winograd B, de Grujil TD, et al. Gamma delta T-cell based cancer immunotherapy: Past-Present-Future. *Front Immunol* (2022) 13:915837/full. doi: 10.3389/fimmu.2022.915837/full
- Yazdanifar M, Barbarito G, Bertaina A, Airolidi I. $\gamma\delta$ T cells: The ideal tool for cancer immunotherapy. *Cells* (2020) 9(5):1305. doi: 10.3390/cells9051305
- Sivan A, Corrales L, Hubert N, Williams JB, Aquino-Michaels K, Earley ZM, et al. Commensal bifidobacterium promotes antitumor immunity and facilitates anti-PD-L1 efficacy. *Science* (2015) 350(6264):1084–9. doi: 10.1126/science.aac4255
- Zitvogel L, Ayyoub M, Routy B, Kroemer G. Microbiome and anticancer immunosurveillance. *Cell* (2016) 165(2):276–87. doi: 10.1016/j.cell.2016.03.001
- Viaud S, Saccheri F, Mignot G, Yamazaki T, Daillère R, Hannani D, et al. The intestinal microbiota modulates the anticancer immune effects of cyclophosphamide. *Science* (2013) 342(6161):971–6. doi: 10.1126/science.1240537
- Routy B, Le Chatelier E, Derosa L, Duong CPM, Alou MT, Daillère R, et al. Gut microbiome influences efficacy of PD-1-based immunotherapy against epithelial tumors. *Science* (2017) 359(6371):91–7. doi: 10.1126/science.aan3706
- Gopalakrishnan V, Spencer CN, Nezi L, Reuben A, Andrews MC, Karpinetz TV, et al. Gut microbiome modulates response to anti-PD-1 immunotherapy in melanoma patients. *Sci* (80-) (2017) 359(6371):97–103. doi: 10.1126/science.aan4236
- Matson V, Fessler J, Bao R, Chongsuwat T, Zha Y, Alegre M-L, et al. The commensal microbiome is associated with anti-PD-1 efficacy in metastatic melanoma patients. *Science* (2018) 359(6371):104–8. doi: 10.1126/science.aao3290
- Ganusov VV, De Boer RJ. Do most lymphocytes in humans really reside in the gut? *Trends Immunol* (2007) 28(12):514–8. doi: 10.1016/j.it.2007.08.009
- Constantinides MG, Belkaid Y. Early-life imprinting of unconventional T cells and tissue homeostasis. *Science* (2021) 374(6573):p1338–1338. doi: 10.1126/science.abf0095
- Vantourout P, Hayday A. Six-of-the-best: Unique contributions of $\gamma\delta$ T cells to immunology. *Nat Rev Immunol* (2013) 13(2):88–100. doi: 10.1038/nri3384
- Willcox BE, Willcox CR. $\gamma\delta$ TCR ligands: The quest to solve a 500-million-year-old mystery. *Nat Immunol* (2019) 20(2):121–8. doi: 10.1038/s41590-018-0304-y
- Holmes E, Li JV, Marchesi JR, Nicholson JK. Gut microbiota composition and activity in relation to host metabolic phenotype and disease risk. *Cell Metab* (2012) 16(5):559–64. doi: 10.1016/j.cmet.2012.10.007
- Gibson GR, Hutkins R, Sanders ME, Prescott SL, Reimer RA, Salminen SJ, et al. Expert consensus document: The international scientific association for probiotics and prebiotics (ISAPP) consensus statement on the definition and scope of prebiotics. *Nat Rev Gastroenterol Hepatol* (2017) 14(8):491–502. doi: 10.1038/nrgastro.2017.75
- Matson V, Fessler J, Bao R, Chongsuwat T, Zha Y, Alegre M-L, et al. The commensal microbiome is associated with anti-PD-1 efficacy in metastatic melanoma patients. *Science* (2018) 359(6371):104–8. doi: 10.1126/science.aao3290
- Li Y, Elmén L, Segota I, Xian Y, Tinoco R, Feng Y, et al. Prebiotic-induced anti-tumor immunity attenuates tumor growth. *Cell Rep* (2020) 30(6):1753–1766.e6. doi: 10.1016/j.celrep.2020.01.035
- Uerlings J, Schroyen M, Willems E, Tanghe S, Bruggeman G, Bindelle J, et al. Differential effects of inulin or its fermentation metabolites on gut barrier and immune function of porcine intestinal epithelial cells. *J Funct Foods* (2020) 67:103855. doi: 10.1016/j.jff.2020.103855
- Meyer D, Stasse-Wolthuis M. The bifidogenic effect of inulin and oligofructose and its consequences for gut health. *Eur J Clin Nutr* (2009) 63(11):1277–89. doi: 10.1038/ejcn.2009.64
- Belkaid Y, Harrison OJ. Homeostatic immunity and the microbiota. *Immunity* (2017) 46(4):562–76. doi: 10.1016/j.immuni.2017.04.008
- Nielsen MM, Witherden DA, Havran WL. $\gamma\delta$ T cells in homeostasis and host defence of epithelial barrier tissues. *Nat Rev Immunol* (2017) 17(12):733–45. doi: 10.1038/nri.2017.101
- Skwarczynski M. Inulin: A new adjuvant with unknown mode of action. *EBioMedicine* (2017) 15:8–9. doi: 10.1016/j.ebiom.2016.11.019
- Rosales-Mendoza S, Salazar-González JA, Decker EL, Reski R. Implications of plant glycans in the development of innovative vaccines. *Expert Rev Vaccines* (2016) 15(7):915–25. doi: 10.1586/14760584.2016.1155987
- Ribas A, Shin DS, Zaretsky J, Frederiksen J, Cornish A, Avramis E, et al. PD-1 blockade expands intratumoral memory T cells. *Cancer Immunol Res* (2016) 4(3):194–203. doi: 10.1158/2326-6066.CIR-15-0210
- Spencer CN, McQuade JL, Gopalakrishnan V, McCulloch JA, Vetizou M, Cogdill AP, et al. Dietary fiber and probiotics influence the gut microbiome and melanoma immunotherapy response. *Science* (2021) 374(6575):1632–40. doi: 10.1126/science.aaz7015
- Chen H, Cong X, Wu C, Wu X, Wang J, Mao K, et al. Intratumoral delivery of CCL25 enhances immunotherapy against triple-negative breast cancer by recruiting CCR9 + T cells. *Sci Adv* (2020) 6(5). doi: 10.1126/sciadv.aax4690
- Simon S, Labarriere N. PD-1 expression on tumor-specific T cells: Friend or foe for immunotherapy? *Oncoimmunology* (2018) 7(1):e1364828. doi: 10.1080/2162402X.2017.1364828
- Hannani D, Ma Y, Yamazaki T, Déchanet-Merville J, Kroemer G, Zitvogel L. Harnessing $\gamma\delta$ T cells in anticancer immunotherapy. *Trends Immunol* (2012) 33(5):199–206. doi: 10.1016/j.it.2012.01.006
- Pallett LJ, Swadling L, Diniz M, Maini AA, Schwabenland M, Gasull AD, et al. Tissue CD14+CD8+ T cells reprogrammed by myeloid cells and modulated by LPS. *Nature* (2023) 614:334–42. doi: 10.1038/s41586-022-05645-6
- Komai-Koma M, Gildchrist DS, Xu D. Direct recognition of LPS by human but not murine CD8+ T cells via TLR4 complex. *Eur J Immunol* (2009) 39(6):1564–72. doi: 10.1002/eji.200838866
- Papotto PH, Yilmaz B, Silva-Santos B. Crosstalk between $\gamma\delta$ T cells and the microbiota. *Nat Microbiol* (2021) 6(9):1110–7. doi: 10.1038/s41564-021-00948-2
- Godon JJ, Zumstein E, Dabert P, Haboubiz F, Moletta R. Molecular microbial diversity of an anaerobic digester as determined by small-subunit rDNA sequence analysis. *Appl Environ Microbiol* (1997) 63(7):2802–13. doi: 10.1128/aem.63.7.2802-2813.1997
- Caporaso JG, Kuczynski J, Stombaugh J, Bittinger K, Bushman FD, Costello EK, et al. QIIME allows analysis of high-throughput community sequencing data. *Nat Methods* (2010) 7(5):335–6. doi: 10.1038/nmeth.f.303
- Escudié F, Auer L, Bernard M, Mariadassou M, Cauquil L, Vidal K, et al. FROGS: Find, rapidly, OTUs with galaxy solution. *Berger B editor Bioinf* (2018) 34(8):1287–94. doi: 10.1093/bioinformatics/btx791
- Bernard M, Rué O, Mariadassou M, Pascal G. FROGS: a powerful tool to analyse the diversity of fungi with special management of internal transcribed spacers. *Brief Bioinform* (2021) 22(6). doi: 10.1093/bib/bbab318/6354026
- McMurdie PJ, Holmes S. Phyloseq: An R package for reproducible interactive analysis and graphics of microbiome census data, in: (2013). Available at: <https://dx.plos.org/10.1371/journal.pone.0061217>.